Optimization of antireflection coating design using pc1d simulation for c − si solar cell application

electronics

MDPI

Article

Optimization of Antireflection Coating Design Using *PC1D* Simulation for $c-Si$ Solar Cell Application

Maruthamuthu Subramanian [1], Omar M. Aldossary [2], Manawwer Alam [3], Mohd Ubaidullah [3], Sreedevi Gedi [4,*], Lakshminarayanan Vaduganathan [5], Gokul Sidarth Thirunavukkarasu [6], Elmira Jamei [7], Mehdi Seyedmahmoudian [6,*], Alex Stojcevski [6] and Saad Mekhilef [6]

1 Department of Physics, PSG Institute of Technology and Applied Research, Coimbatore 641062, India; maruthamuthu@psgitech.ac.in
2 Department of Physics and Astronomy, College of Science, King Saud University, Riyadh 11451, Saudi Arabia; omar@ksu.edu.sa
3 Department of Chemistry, College of Science, King Saud University, Riyadh 11451, Saudi Arabia; maalam@ksu.edu.sa (M.A.); mtayyab@ksu.edu.sa (M.U.)
4 School of Chemical Engineering, Yeungnam University, Gyeongsan 38541, Korea
5 Department of Electrical and Electronics Engineering, Dr. Mahalingam College of Engineering and Technology, Pollachi 642003, India; vlnaarayan@gmail.com
6 School of Science, Computing and Engineering Technologies, Swinburne University of Technology, Melbourne, VIC 3122, Australia; gthirunavukkarasu@swin.edu.au (G.S.T.); astojcevski@swin.edu.au (A.S.); smekhilef@swin.edu.au (S.M.)
7 College of Engineering and Science, Victoria University, Melbourne, VIC 3011, Australia; Elmira.jamei@vu.edu.au
* Correspondence: drsrvi9@gmail.com (S.G.); mseyedmahmoudian@swin.edu.au (M.S.)

check for updates

Citation: Subramanian, M.; Aldossary, O.M.; Alam, M.; Ubaidullah, M.; Gedi, S.; Vaduganathan, L.; Thirunavukkarasu, G.S.; Jamei, E.; Seyedmahmoudian, M.; Stojcevski, A.; et al. Optimization of Antireflection Coating Design Using *PC1D* Simulation for $c-Si$ Solar Cell Application. *Electronics* **2021**, *10*, 3132. https://doi.org/10.3390/electronics10243132

Academic Editors: Hani Vahedi, Edris Pouresmaeil, Kent Bertilsson and Emad Samadaei

Received: 20 October 2021
Accepted: 30 November 2021
Published: 16 December 2021

Publisher's Note: MDPI stays neutral with regard to jurisdictional claims in published maps and institutional affiliations.

Abstract: Minimizing the photon losses by depositing an anti-reflection layer can increase the conversion efficiency of the solar cells. In this paper, the impact of anti-reflection coating (ARC) for enhancing the efficiency of silicon solar cells is presented. Initially, the refractive indices and reflectance of various ARC materials were computed numerically using the $OPAL2$ calculator. After which, the reflectance of SiO_2, TiO_2, $SiNx$ with different refractive indices (n) were used for analyzing the performance of a silicon solar cells coated with these materials using $PC1D$ simulator. SiN_x and TiO_2 as single-layer anti-reflection coating $(SLARC)$ yielded a short circuit current density (J_{sc}) of 38.4 mA/cm^2 and 38.09 mA/cm^2 respectively. Highest efficiency of 20.7% was obtained for the SiN_x ARC layer with $n = 2.15$. With Double-layer anti-reflection coating $(DLARC)$, the J_{sc} improved by $\sim$0.5 mA/cm^2 for SiO_2/SiN_x layer and hence the efficiency by 0.3%. Blue loss reduces significantly for the $DLARC$ compared with $SLARC$ and hence increase in J_{sc} by 1 mA/cm^2 is observed. The J_{sc} values obtained is in good agreement with the reflectance values of the ARC layers. The solar cell with $DLARC$ obtained from the study showed that improved conversion efficiency of 21.1% is obtained. Finally, it is essential to understand that the key parameters identified in this simulation study concerning the $DLARC$ fabrication will make experimental validation faster and cheaper.

Keywords: anti-reflection coating; crystalline silicon; solar cells; $PC1D$; $OPAL2$

1. Introduction

With the substantial technological advancements, the potential for high conversion efficiency of crystalline silicon $(c-Si)$ solar cells. Photovoltaic (PV) market dominated by crystalline silicon $(c-Si)$ solar cells [1] by larger than 90% worldwide. The efficiency of 24.4% has been reached with $c-Si$ based modules and is continuously escalating both in the research and in the commercial market. Theoretically, the bandgap, long radiative recombination lifetimes, Auger recombination of the generated carriers restrict the conversion efficiency to about 29% [2–4]. It is mandatory to reduce the various losses (optical, carrier, and electrical loss) in $c-Si$ solar cell to achieve the maximum conversion

efficiency [5]. One of the key issues of the contemporary PV industry is reducing the optical losses which make up about 4% efficiency loss in $c-Si$ solar cells [6]. An approach to reduce the optical loss is to use an ARC at the front surface, which reduces the reflection losses and enhances the J_{sc} consequently, improving the conversion efficiency. Several researchers employed various ARCs that might be used to increase the efficiency of the solar cell. Thin films such as TiO_2, SiO_2, SiN_x, Al_2O_3 etc., were used as ARC layers [7–11]. TiO_2 was a commonly used ARC on the front surface, owing to its versatility and inexpensive [7]. Though TiO_2 coatings possess better optical properties (high refractive index, low absorption coefficient) in the visible region, the passivation properties in addition to the optical properties made the PV manufacturers shift to plasma-enhanced chemical vapour deposited $(PECVD)$ SiN_x. In the recent study by various researchers, TiO_2 films demonstrated the potential of delivering the exceptional passivation on boron-doped (p^+) emitters [12–14]. TiO_2 is the ideal ARC material for the encapsulated cell as its $n = \sim 2.1$ at the wavelength of 630 nm. In the earlier days of solar cell fabrication, TiO_2 was considered only for ARC purposes. Later researchers found that SiO_2/SiN_x layers provided both surface passivation as well as ARC layers. Hence the solar cell industry utilizes the SiO_2/SiN_x layers. However recent research found the passivation properties especially provided better surface passivation with p^+ surfaces. However, the change in its crystalline phase at higher temperatures hinders the application of TiO_2 in conventional commercial solar cells fabrication, which requires high-temperature metallisation firing. Hence it might be considered. Thus, optimizing the TiO_2 film with a trade-off between optical and passivation properties will be valuable for the PV industry.

However, the single-layer ARCs $(SLARC)$ employed in silicon solar cells still instigate substantial optical reflectance loss in a wide-ranging of the solar spectrum. Thus, high-efficiency solar cells utilize double-layer ARCs $(DLARC)$ which improves the carrier collection by reducing the reflectance in the visible and in the near-IR range [15–18]. The $DLARC$ (SiO_2/TiO_2 or SiO_2/SiO_x) is a favorable design to enhance the efficiency owing to its benefits in both antireflection and surface passivation properties. Doshi et.al. optimized the ARC film thickness and their refractive indices and utilized the SiO_2/SiN_x $DLARC$ for their simulation [15]. With SiO_2/SiN_x $DLARC$ layer, Lennie et al. obtained an efficiency of 4.56% [16] using Silvaco ATLAS simulation. Similar work with $PC1D$ simulation can be found elsewhere [17–19]. $PC1D$ is the most commercially accessible software utilized by several groups to simulate solar cells with unique ARC layers [20]. In most of the ARC simulation studies, the maximum conversion efficiency of 3–13% only has been achieved [16–19].

In the present study, we employed the $SLARC$ and $DLARC$ on the actual industrial solar cell with a surface area of 244.32 cm^2. Similarly, we analyzed the ARC loss for each ARC layer, to find the most optimum ARC specification that can be employed for solar cell application. For $DLARC$, varying the thickness of the SiO_2 and its capping layer was one of the most novel concepts explored in this manuscript. This simulation-based approach highlighted in this manuscript plays a vital role in identifying the most optimal configuration of the ARC layers for achieving increased efficiency of silicon solar cells. The simulation approach highly reduces the time and cost involved in testing the different combinations of $DLARC$ layers and helps in identifying the optimal configuration of the ARC layers. SiN_x with different refractive indices were chosen as a capping layer when experimentally testing the $DLARC$ layer. Mono-crystalline silicon solar cells were simulated using $PC1D$. The simulated device results were validated by comparing the solar cell fabricated with identical device parameters. This study offers a better insight into solar cell performance.

2. Simulation of $c-Si$ Solar Cell

To simulate the $c-Si$ solar cell behaviour $PC1D$ software package is used in this study. The mathematical modelling tool used a more detailed silicon solar cell model as shown in Figure 1. To increase the conversion accuracy of solar cells we need an accurate solar cell

modelling tool. After studying each layer's physical and electrical parameters of the $c-Si$ solar cell the $PC1D$ tool helps in studying the impact of various parameters considered in the fabrication of the solar cells. In this study, the actual device configuration for simulating and optimizing the anti-reflection coating (ARC) layer of solar cell is evaluated using $PC1D$ simulation and the optimized configuration for achieving higher accuracy is obtained. Using numerical modelling tools such as $PC1D$ to optimize the ARC layer configurations reduces the cost, time, and effort required to analyze the impact of the change in the design of the solar cells.

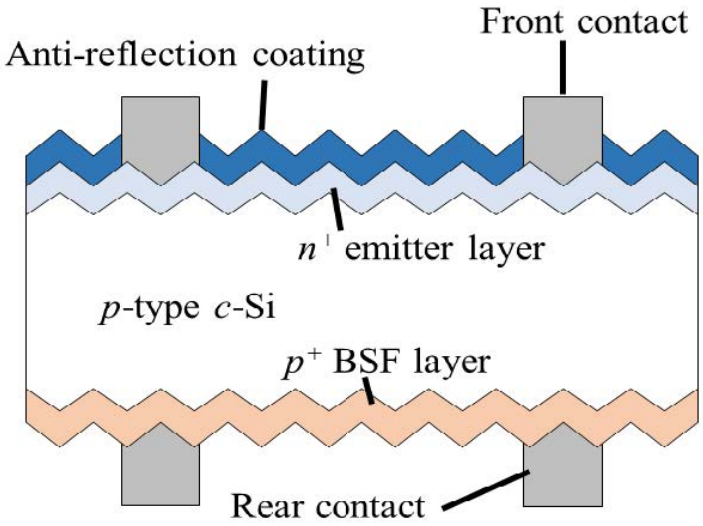

Figure 1. Silicon solar cell structure used for this study.

In the $PC1D$ simulation tool, crystalline Si $(c-Si)$ solar cell device simulations are carried out using the following numerical equations representing the quasi-one-dimensional transportation of electrons and holes of a semiconductor material (Solar cells). Equations (1)–(7) gives us a clear cut idea of creating a model of a silicon cell and optimizing various process parameters including the ARC coating layer properties [21].

$$J_n = \mu_n \cdot n \cdot \bigtriangledown E_{Fn} \tag{1}$$

$$J_p = \mu_p \cdot p \cdot \bigtriangledown E_{Fp} \tag{2}$$

The current densities of the electrons and the holes are represented as J_n and J_p respectively and they are numerically formulated as indicated in Equations (1) and (2). In which, the parameters n and p are the electron and hole density, μ_n and μ_p is the mobility of the electron and holes. The $\bigtriangledown E_{Fn}$ and $\bigtriangledown E_{Fp}$ are the diffusion coefficients that represents the difference in electron and hole quasi-Fermi energies E_{Fn} and E_{Fp}.

$$\frac{\partial n}{\partial t} = \frac{\bigtriangledown \cdot J_n}{q} + G_L - U_n \tag{3}$$

$$\frac{\partial p}{\partial t} = \frac{\bigtriangledown \cdot J_p}{q} + G_L - U_p \tag{4}$$

$$\Delta^2 \phi = \frac{q}{\epsilon}\left(n - p + N_{acc}^- - N_{don}^+\right) \tag{5}$$

Equations (3) and (4) are derived from the law of conservation of charge or the continuity equation. where G_L and U_n are generation rate and recombination rate. Equation (5) represents Poisson's equation for solving the electrostatic field problems. where N_{acc}^{-} and N_{don}^{+} are acceptor and donor doping concentrations.

$$n = N_C F_{1/2}\left(\frac{q\psi + V_n - q\phi_{n,i} + \ln\left(n_{i,0}/N_C\right)}{k_B T}\right) \tag{6}$$

$$p = N_V F_{1/2}\left(\frac{-q\psi + V_p - q\phi_{p,i} + \ln\left(n_{i,0}/N_V\right)}{k_B T}\right) \tag{7}$$

Here N_c and N_v are the effective density of states in the conduction and valence bands. To describe the type of material used, Fermi-Dirac statistics directly related to the band edges and N_c and N_v carrier densities are expressed in the Equations (7) and (8). The finite element approach is used to solve the three basic equations that assist in simulating the solar cell behaviours using the *PC*1*D* modelling tool. Many other process parameters are optimized using the *PC*1*D* simulation tool in the literature, but the proposed research aims to optimise the design process characteristics of the *ARC* layer used in the fabrication of the $c - Si$ solar cells. Finally, the efficiency of $c - Si$ solar cells is calculated using the following equations.

$$\eta = \frac{P_{\max}}{I_{\text{in}}} = \frac{J_{\text{mpp}} V_{\text{mpp}}}{I_{\text{in}}} = \frac{J_{\text{SC}} V_{\text{OC}} FF}{I_{\text{in}}} \tag{8}$$

where, η represents the efficiency of the solar cell which is calculated using $P_{\max}$, I_{in}, J_{mpp}, V_{mpp}, J_{SC}, V_{OC} and FF that indicates the maximum power, incident power, current at maximum power point, voltage at maximum power point, saturation current density, Open circuit voltage and fill factor.

In this present study, we have considered p-type wafer with resistivity of $1\ \Omega - \text{cm}$ (doping of $1.5 \times 10^{16}\ \text{cm}^3$), device area of $244.32\ \text{cm}^2$, front surface textured with $3\ \mu\text{m}$ depth. The n^+ emitter and p^+ back surface field was formed with doping concentration of $1 \times 10^{20}\ \text{cm}^{-3}$ and $3 \times 10^{18}\ \text{cm}^{-3}$ respectively. Bulk lifetime of $100\ \mu\text{s}$ and front and rear surface recombination velocity of $10{,}000\ \text{cm/s}$ were considered for solar cell simulation by PC1D. Numerous simulations were performed to study the impact of different parameters on the solar cell device performance. Base resistance $(0.015\ \Omega)$, internal conductance $(0.3\ \text{S})$, light intensity $(0.1\ \text{W/cm}^2)$ were kept constant during simulation. *AM*1.5*G* spectrum was used in this modelling.

3. Results and Discussion

The refractive index as a function of wavelength defines the characteristics of an *ARC* layer [22]. Figure 2 shows the wavelength dependent refractive indices of the *ARC* layers such as TiO_2 [14], MgF_2 [23], SiO_2 [24], SiN_x [9] thin films determined using the spectroscopic ellipsometer. The inset of Figure 2 shows the refractive index corresponding to each *ARC* layer. The refractive index values of the $TiO_2, MgF_2, SiO_2, SiN_x - A, B$ and C at 600 nm were about 2.28 2.34, 1.36, 1.46, 1.99, 2.15, and 2.17 respectively.

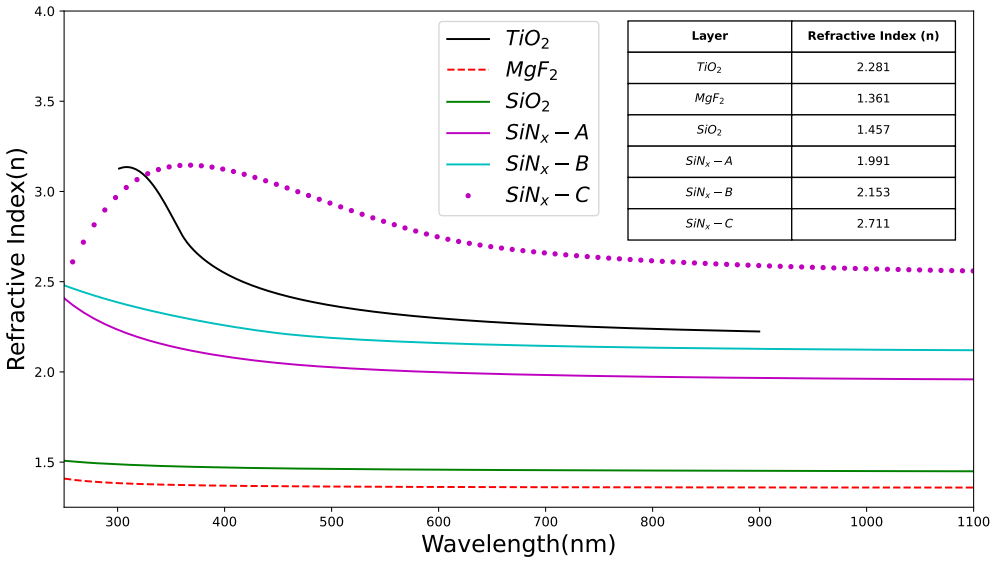

Layer	Refractive Index (n)
TiO_2	2.281
MgF_2	1.361
SiO_2	1.457
$SiN_x - A$	1.991
$SiN_x - B$	2.153
$SiN_x - C$	2.711

Figure 2. Refractive indices of various *ARC* layers.

Reflectance spectra as a function of wavelength feed significant insights that can be used for investigating the optical properties of the *ARC*, textured surface, and internal reflectance at the rear surface of the solar cell device. An optimal *ARC* film for $c - Si$ solar cells should possess (i) low optical losses and (ii) provide good surface passivation. Reflectance spectra exhibit characteristic minima that are defined by the following equation:

$$t = \frac{\lambda_0}{4n} \tag{9}$$

where t represents the thickness of the *ARC*, λ_0 represents the characteristic minimum wavelength, and n represents the index of refraction. For each *ARC* layer with a different refractive index, the thickness of the *ARC* layer was varied from 70–100 nm to keep the optical thickness of the film constant. Figure 3 shows the measured reflectance of the different *ARC* layers coated on the textured surface. These reflectance values were measured using *OPAL*2 software. The *OPAL*2 simulator was also used to optimise the layer thickness of the single/double-layer *ARC* coatings. The reflectance values were measured at the wavelength of 630 nm. The reflectance of *ARC* layers such as $TiO_2, MgF_2, SiO_2, SiN_x - A, SiN_x - B$ and $SiN_x - C$ are 0.29%, 0.46%, 4.18%, 0.88%, 0.045%, 0.08% and 1.55% respectively. Overall, the lowest reflectance value is for $Sin_{x-A}(n = 1.99)$ and $Sin_x - B(n = 2.15)$ *ARC* layer, closely followed by $TiO_2(n = 1.99)$. Similar behaviour is observed in the case of saturation current density (J_{sc}). Table 1 represents the $I - V$ parameters as well as the calculated blue loss and *ARC* loss with different *SLARC* layers J_{sc} of 38.37 mA/cm^2, 38.4 mA/cm^2 was obtained for $SiN_x - A$ $(n = 1.99)$ and $SiN_x - B$ $(n = 2.15)$ *ARC* layer and 38.16 mA/cm^2 and 38.09 mA/cm^2 for TiO_2 $(n = 1.99)$ respectively. The J_{sc} values obtained is in good agreement with the reflectance values of the *ARC* layers. Highest efficiency of 20.7% was obtained for the SiN_x *ARC* layer with $n = 1.99$ and 2.15. Current is one of the easiest factor that can be improved with substantial margin. Thus it is significant to enumerate systematically the source of J_{sc} loss, breaking them into (i) optical losses and (ii) collection losses. The optical loss is due to metal shading, reflection and parasitic absorption and the collection losses arises due to imperfect emitter collection. By investigating the losses, it gives a clear representation of possible improvement areas which helps the PV manufacturers to predict and plan the strategies on the cell and module level fabrication for the future. Despite the well-known fact that the Mg-based *ARC* material is considered as the highly impactful material its associated drawback in terms of the J_{SC} loss was highlighted and alternative materials J_{SC} loss was evaluated and a detailed overview of the results was presented in Table 2.

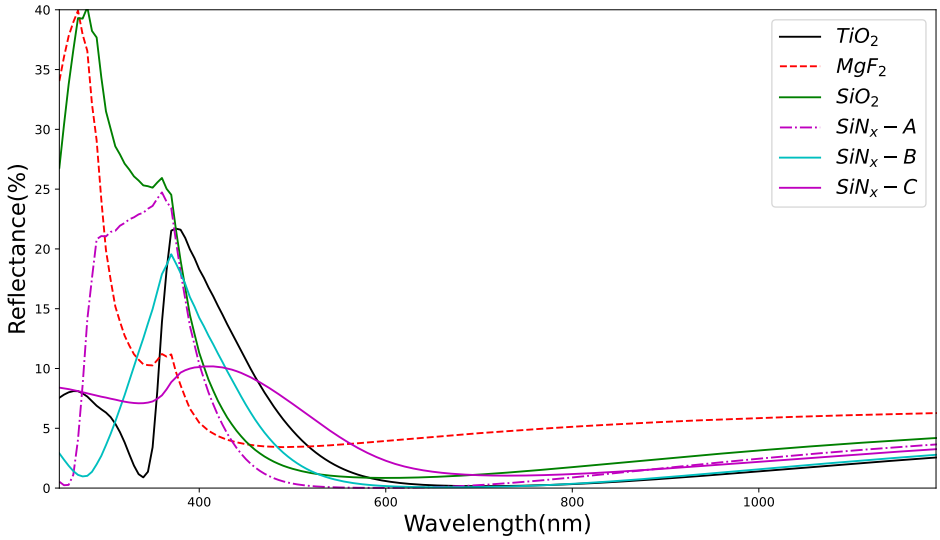

Figure 3. Reflectance spectra as a function of wavelength for some optimised single-layer anti-reflection coating.

Table 1. $I - V$ parameters and ARC loss calculation based on the different SLARC layers.

ARC Layer	J_{sc} (mA/cm^2)	V_{oc} (mV)	*FF* (%)	Eff (%)	Blue Loss (%)	*ARC* Loss [%]	Unshaded J_{sc} (mA/cm^2)
TiO_2	38.16	654.2	82.42	20.58	0.17	1.74	39.35
MgF_2	37.27	653.5	82.45	20.08	0.17	1.81	39.29
SiO_2	38.0	653.9	82.43	20.48	0.17	1.34	39.75
$SiN_x - A$	38.37	654.1	82.42	20.69	0.17	0.90	40.18
$SiN_x - B$	38.4	654.3	82.42	20.71	0.17	1.25	39.83
$SiN_x - C$	37.79	653.7	82.43	20.37	0.17	1.95	39.13

Table 2. $I - V$ parameters of the different $DLARC$ layers.

ARC Layer	J_{sc} (mA/cm^2)	V_{oc} (mV)	*FF* (%)	Eff (%)	Blue Loss (%)	*ARC* Loss [%]	Unshaded J_{sc} (mA/cm^2)
$SiO_2 - TiO_2$	30.84	648.6	82.59	16.52	0.13	10.39	30.83
$SiO_2 - MgF_2$	37.75	653.9	82.43	20.35	0.13	2.52	38.65
$SiO_2 - SiN_x - A$	33.16	650.5	82.54	17.8	0.13	8.70	32.50
$SiO_2 - SiN_x - B$	31.87	649.4	82.57	17.09	0.13	9.48	31.72
$SiO_2 - SiN_x - C$	29.48	647.4	82.61	15.76	0.13	8.91	32.30

To explain the variation in the J_{sc} with different ARC layers, the ARC loss was calculated by considering the $AM1.5G$ photon flux spectrum [25] and internal quantum efficiency of the solar cell.

$$J_{sc} = q \int I_{AM1.5}(\lambda)[1 - R(\lambda)] \cdot \mathrm{IQE}(\lambda) d\lambda \tag{10}$$

where q is the elementary charge, lam $1.5(\lambda)$ denotes the photon flux of the standard air mass solar spectrum between 300 to 1100 nm, $\mathrm{R}(\lambda)$ is the reflectance and $\mathrm{IQE}(\lambda)$ is the internal quantum efficiency as a function of wavelength.

Reflection loss lead to a reduction of 2 mA/cm^2 in J_{sc} for TiO_2, MgF_2 layers, 1.5 mA/cm^2 for thermal SiO_2, 1.07, 1.42 and 2.12 mA/cm^2 for SiN_x layers with different refractive indices, thus decreasing the efficiency with respective ARC layers. The front metal coverage is not considered while calculating the J_{sc} values and hence, the variation. By considering the metal coverage area (4–7%), the calculated unshaded J_{sc} values is in good agreement with the measured J_{sc}.

This ARC loss may be reduced by tuning the ARC optical properties (e.g., refraction index and thickness), as well as through improved front surface texturing for better light-trapping. In general, the optical properties of the ARC materials are modified by replacing them with an alternate material to be used as the ARC material. One other alternate way of reducing the ARC loss is by optimizing the refractive indices of the ARC layer. In this study, SiN_x layers have been used with different refractive indices from n = 1.99; 2.15 and 2.711 to analyse the impact of the material used as the ARC in the manuscript. From Table 1 it is inferred that the ARC loss was higher for the SiN_x layers with the highest refractive indices, and it reduces significantly with a reduction in the refractive indices. The blue loss is the combined effect of ARC absorption, imperfect emitter collection, and front surface recombination. ARC-related blue loss may be reduced to a certain extent by tuning the ARC optical properties. Optimizing the emitter doping profile and junction depth can also help reduce emitter recombination losses. Front surface recombination can be reduced by improved front surface passivation.

For further reduction in the reflectance, we considered the $DLARC$. Figure 4 depicts the reflectance spectra of various $DLARC$ layers. The SiO_2 layer was capped with MgF_2, TiO_2 and SiN_x layers. The thickness of the SiO_2 layer and the capping layers were fixed as 100 nm and 80 nm respectively. The reflectance was higher for all the $DLARC$ layers and hence poor J_{sc} values which are depicted in Table 2. The high reflectance values for all the $DLARC$ layers are attributed to the unequal optical thickness of the $DLARC$ layer. The necessary and sufficient refractive index condition for a $DLARC$ with equal optical thickness to give zero reflectance is [26]:

$$\frac{n_1}{n_2} = \sqrt{\frac{n_0}{n_s}} \tag{11}$$

where n_0 is the admittance of the surrounding medium.

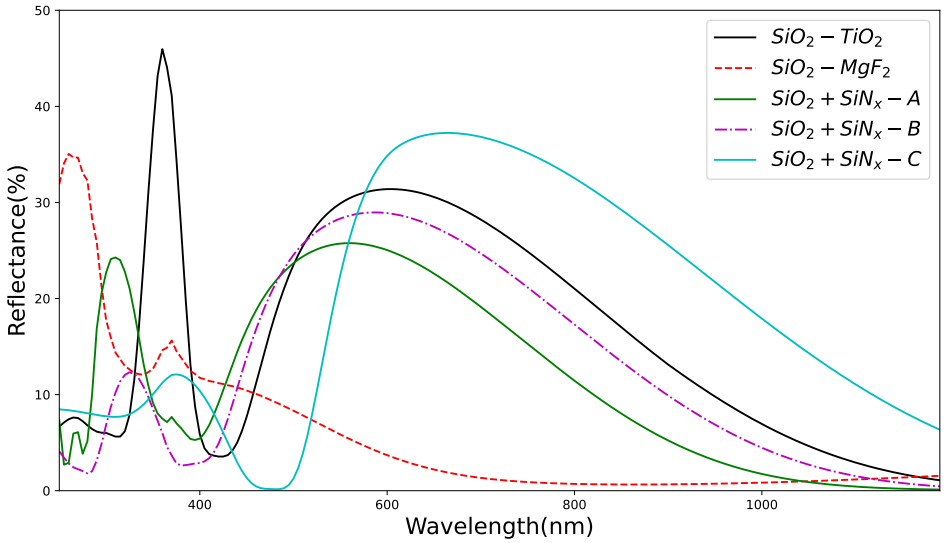

Figure 4. Reflectance spectra as a function of wavelength for some double-layer anti-reflection coating.

Based on Equation (11) the optical thickness of the $DLARC$ layers was optimized to obtain a minimum reflectance. Figure 5 shows the reflectance spectra of the $DLARC$ layers. The inset of Figure 6 shows the thickness variation for both SiO_2 and the capping layer. The SiO_2 layer capped with MgF_2 and SiN_{x-C} $(n = 2.71)$ showed a reflectance of 2.2% whereas for the TiO_2, $SiN_x - A$ and $SiN_x - B$ layers the reflectance was 0.34%, 0.11% and 0.19% respectively with the thickness of ~60–70 nm. From the optimized reflectance curves, we can observe that when the reflectivity is substantially mitigated at the front surface, the gain in efficiency of the solar cell. Table 3 represents the $I - V$ parameters as well as the calculated blue loss and ARC loss with optimized $DLARC$ layers. With

DLARC, the J_{sc} improved by $\sim$0.5 mA/cm^2 when the SiO_2 was capped with SiN_x layer and hence the efficiency by 0.3%. It can be observed that the blue loss reduces significantly for the *DLARC* compared with *SLARC*. This reduction can be attributed to the effective passivation provided by the SiO_2 layer. With *DLARC*, the reflection loss reduced by 50% i.e., $\sim$1 mA/cm^2 in J_{sc}compared with *SLARC*.

Table 3. $I-V$ parameters and *ARC* loss calculation based on the optimized *DLARC* layers.

ARC Layer	J_{sc} (mA/cm^2)	V_{oc} (mV)	*FF* (%)	Eff (%)	Blue Loss (%)	*ARC* Loss [%]	Unshaded J_{sc} (mA/cm^2)
SiO_2-TiO_2	38.29	654.2	82.42	20.65	0.13	1.03	40.13
SiO_2-MgF_2	38.11	654.1	82.43	20.55	0.13	1.42	39.74
SiO_2-SiN_x-A	38.41	654.3	82.42	20.72	0.13	0.83	40.34
SiO_2-SiN_x-B	38.52	654.4	82.42	20.78	0.13	0.67	40.49
SiO_2-SiN_x-C	38.16	654.1	82.42	20.57	0.13	1.03	40.13

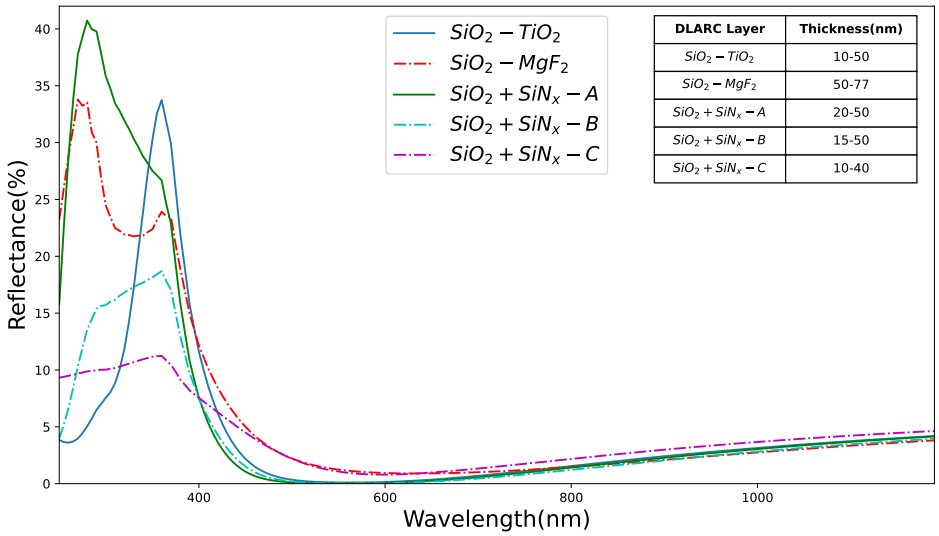

Figure 5. Reflectance spectra as a function of wavelength with optimized thickness of double-layer anti-reflection coating.

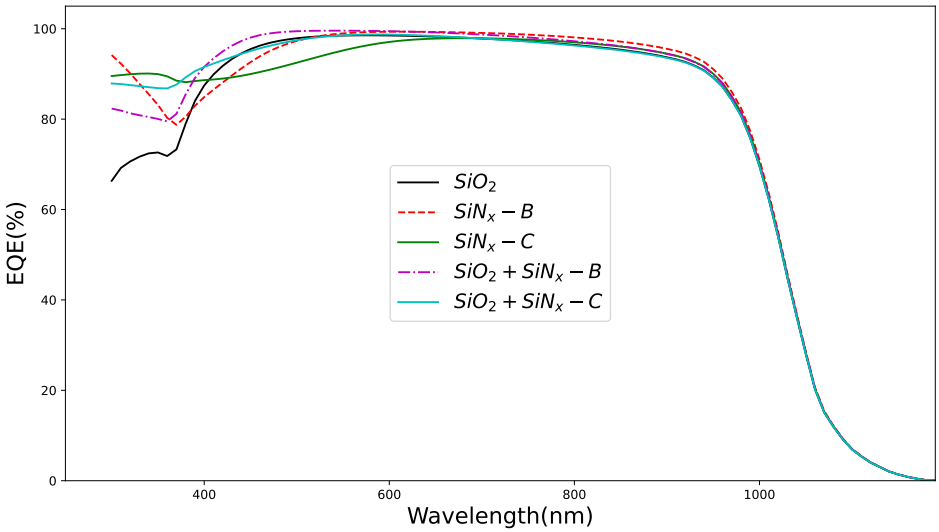

Figure 6. *EQE* measurement carried on selected *ARC* layers.

Figure 6 depicts the EQE obtained on the selected ARC layers. *SLARC* of SiO_2 layer showed a better blue response compared with SiN_x-B layers. However, the increase in

J_{sc} for the $SiN_x - B$ layers is due to the better response i.e., more absorption in the long-wavelength region. From Figure 6 it is obvious that with the utilization of the $DLARC$ layer, the carrier collection has improved significantly in the short wavelength range leading to the best conversion efficiency and J_{sc}. This enhancement in EQE is attributed to the decrease in reflection with $DLARC$. It is sufficient to say, this effective collection of carriers reduce the recombination at the interface, and hence the overall EQE is enhanced [10].

To validate the simulation data, a simulated device with identical parameters was compared to the measurements of actual solar cells in real application conditions. The industrial silicon solar cell was fabricated with both $SLARC$ and $DLARC$. 55 nm thick SiO_x layer with the refractive index of 2.05 was used as $SLARC$ layer. SiO_2 with 15 nm thick and SiN_x with 70 nm thick were used as $DLARC$ layer. The monocrystalline silicon solar cell showed the conversion efficiency of 20.8% and 21.1% shown in the inset of Figure 7. EQE spectra indicate that the efficiency improvement for a solar cell with the $DLARC$ compared to the $SLARC$. This improvement at the short wavelength region is vital and it's attributed mainly to the role of the $DLARC$. Thus, the SiO_2/SiN_x stacked layers reduce the reflection of high energy photons. In addition, the ARC layers provide better passivation thus enhancing the overall EQE by reducing the surface recombination at the interface. The efficiency of the solar cell using the optimized ARC layer settings is compared with the results obtained from the literature and presented in Table 4. The result indicated that the identified ARC layer configuration outperforms the previously identified $SLARC$ and $DLARC$ layers highlighted in the literature.

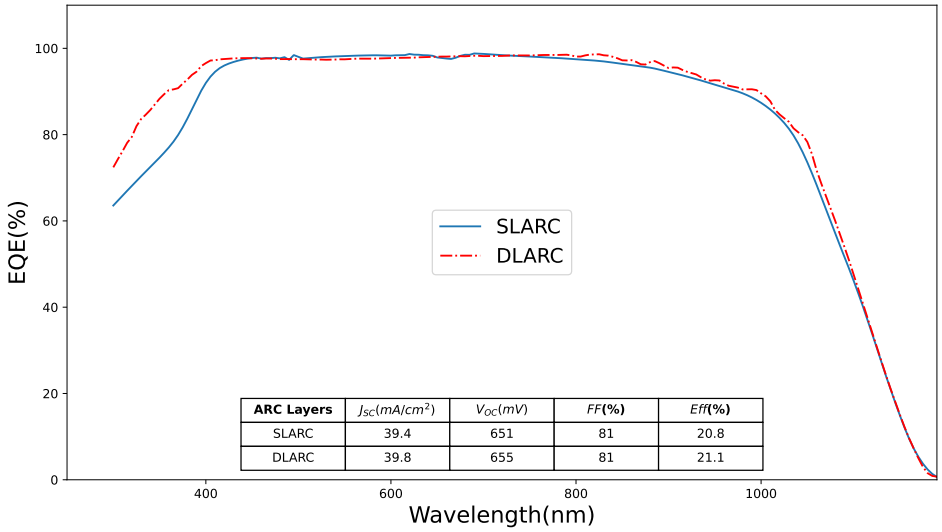

Figure 7. EQE measurement carried on single and double layer ARC layers. Inset shows the IV results obtained with the solar cell measurement.

Table 4. Comparison of the $I - V$ results obtained with different ARC layers

Layer Type		Eff (%)	Reference
$SLARC$	SiO_2	18.3	[27]
	SiN_x	19.6	[18]
	SiN_x	20.35	[17]
	SiN_x	20.8	This article
$DLARC$	SiO_2/SiN_x	4.56	[18]
	SiN_x/SiN_x	17.8	[28]
	SiO_2/SiO_xN_y	18.59	[27]
	SiO_2/SiN_x	18.62	[29]
	SiN_x/SiN_x	20.22	[19]
	SiN_x/SiN_x	20.67	[17]
	SiN_x/SiN_x	21.1	This Article

4. Conclusions

The impact of different anti-reflective coating layers on improving the efficiency of silicon solar cells has been studied in this manuscript. Initially, *OPAL*2 simulator was used to compute the refractive indices and reflectance of SiO_2, TiO_2 and SiN_x as *ARC* materials. The calculated reflectance value of the *ARC* material was later used in analyzing its performance on the silicon solar cells using *PC*1*D* software. The impact of the ARC as single and double-layered *ARC* was studied in this research and results indicated that the SiN_x and TiO_2 as *SLARC* yielded a J_{sc} of 38.4 mA/cm^2 and 38.09 mA/cm^2 respectively. Highest efficiency of 20.7% was obtained for the SiN_x *ARC* layer with $n = 2.15$. SiO_2 layer capped with TiO_2, and SiN_x layers showed the lowest reflectance of 0.34% and 0.11% respectively. SiO_2/SiN_x *DLARC* layer increases the J_{sc} by 0.5 mA/cm^2; thereby by increasing the efficiency by 0.3%. The increase in J_{sc} by 1 mA/cm^2 for *DLARC* is attributed to significant reduction in blue loss compared with *SLARC*.

Therefore, it is clear from the observation that the use of *DLARC* over *SLARC* will be advocated considering the impact of increased efficiency and reduced blue loss. This enhancement in EQE for the *DLARC* is attributed to the decrease in reflection as well as a decrease in recombination at the interface. The J_{sc} values obtained is in good agreement with the reflectance values of the *ARC* layers. Further research insights would be targeted towards experimentally evaluating the simulation results on the impact of identified *ARC* layers with silicon solar cell efficiency. The simulation approach highlighted in this manuscript has a bigger advantage in terms of reducing the cost and time required for identifying the best-suited combination of ARC layers that can be considered for the silicon solar cells with *DLARC* finally resulting in higher efficiency. Future research can be benefited from the methodology used in the simulation study to identify the impact of new materials in *DLARC* or *SLARC* fabrication or to identify the optimized parameters required for the fabrication of the silicon solar cells.

Author Contributions: Conceptualization, M.S. (Maruthamuthu Subramanian), O.M.A. and S.G.; methodology, M.A., M.U. and M.S. (Maruthamuthu Subramanian); software, O.M.A., G.S.T. and E.J.; validation, M.S. (Maruthamuthu Subramanian), O.M.A., L.V., S.G. and M.S. (Mehdi Seyedmahmoudian); formal analysis, G.S.T.; investigation, M.A., S.G. and M.U.; resources, M.S. (Maruthamuthu Subramanian) and O.M.A.; data curation, G.S.T., E.J. and M.S. (Mehdi Seyedmahmoudian); writing—original draft preparation, S.G., M.S. (Maruthamuthu Subramanian) and G.S.T.; writing—review and editing, E.J., M.S. (Mehdi Seyedmahmoudian), A.S., M.A., M.U. and S.M.; visualization, G.S.T., E.J., L.V. and M.S. (Mehdi Seyedmahmoudian). All authors have read and agreed to the published version of the manuscript.

Funding: Project Grant (RSP-2021/61), King Saud University, Riyadh, Saudi Arabia.

Institutional Review Board Statement: Not applicable.

Informed Consent Statement: Not applicable.

Acknowledgments: The authors extend their sincere appreciation to the Researchers Supporting Project number (RSP-2021/61), King Saud University, Riyadh, Saudi Arabia for the financial support.

Conflicts of Interest: The authors declare no conflict of interest.

References

1. Andreani, L.C.; Bozzola, A.; Kowalczewski, P.; Liscidini, M.; Redorici, L. Silicon solar cells: Toward the efficiency limits. *Adv. Phys. X* **2019**, *4*, 1548305. [CrossRef]
2. Tiedje, T.; Yablonovitch, E.; Cody, G.D.; Brooks, B.G. Limiting efficiency of silicon solar cells. *IEEE Trans. Electron Devices* **1984**, *31*, 711–716. [CrossRef]
3. Green, M.A. Limits on the open-circuit voltage and efficiency of silicon solar cells imposed by intrinsic Auger processes. *IEEE Trans. Electron Devices* **1984**, *31*, 671–678. [CrossRef]
4. Saga, T. Advances in crystalline silicon solar cell technology for industrial mass production. *NPG Asia Mater.* **2010**, *2*, 96–102. [CrossRef]
5. Tavkhelidze, A.; Bibilashvili, A.; Jangidze, L.; Gorji, N.E. Fermi-Level Tuning of G-Doped Layers. *Nanomaterials* **2021**, *11*, 505. [CrossRef] [PubMed]

6. Smith, D.D.; Cousins, P.; Westerberg, S.; De Jesus-Tabajonda, R.; Aniero, G.; Shen, Y.C. Toward the practical limits of silicon solar cells. *IEEE J. Photovolt.* **2014**, *4*, 1465–1469. [CrossRef]
7. Richards, B. Comparison of TiO_2 and other dielectric coatings for buried-contact solar cells: A review. *Prog. Photovolt. Res. Appl.* **2004**, *12*, 253–281. [CrossRef]
8. Aberle, A.G.; Hezel, R. Progress in low-temperature surface passivation of silicon solar cells using remote-plasma silicon nitride. *Prog. Photovolt. Res. Appl.* **1997**, *5*, 29–50. [CrossRef]
9. Duttagupta, S.; Ma, F.; Hoex, B.; Mueller, T.; Aberle, A.G. Optimised antireflection coatings using silicon nitride on textured silicon surfaces based on measurements and multidimensional modelling. *Energy Procedia* **2012**, *15*, 78–83. [CrossRef]
10. Ju, M.; Balaji, N.; Park, C.; Nguyen, H.T.T.; Cui, J.; Oh, D.; Jeon, M.; Kang, J.; Shim, G.; Yi, J. The effect of small pyramid texturing on the enhanced passivation and efficiency of single c-Si solar cells. *RSC Adv.* **2016**, *6*, 49831–49838. [CrossRef]
11. Remache, L.; Mahdjoub, A.; Fourmond, E.; Dupuis, J.; Lemiti, M. Influence of PECVD SiOx and SiNx: H films on optical and passivation properties of antireflective porous silicon coatings for silicon solar cells. *Phys. Status Solidi C* **2011**, *8*, 1893–1897. [CrossRef]
12. Thomson, A.F.; McIntosh, K.R. Light-enhanced surface passivation of TiO_2-coated silicon. *Prog. Photovolt. Res. Appl.* **2012**, *20*, 343–349. [CrossRef]
13. Liao, B.; Hoex, B.; Shetty, K.D.; Basu, P.K.; Bhatia, C.S. Passivation of boron-doped industrial silicon emitters by thermal atomic layer deposited titanium oxide. *IEEE J. Photovolt.* **2015**, *5*, 1062–1066. [CrossRef]
14. Cui, J.; Allen, T.; Wan, Y.; Mckeon, J.; Samundsett, C.; Yan, D.; Zhang, X.; Cui, Y.; Chen, Y.; Verlinden, P.; et al. Titanium oxide: A re-emerging optical and passivating material for silicon solar cells. *Sol. Energy Mater. Sol. Cells* **2016**, *158*, 115–121. [CrossRef]
15. Doshi, P.; Jellison, G.E.; Rohatgi, A. Characterization and optimization of absorbing plasma-enhanced chemical vapor deposited antireflection coatings for silicon photovoltaics. *Appl. Opt.* **1997**, *36*, 7826–7837. [CrossRef]
16. Lennie, A.; Abdullah, H.; Shila, Z.; Hannan, M. Modelling and simulation of SiO/Si N as anti-reflecting. *World Appl. Sci. J.* **2010**, *11*, 786–790.
17. Hashmi, G.; Rashid, M.J.; Mahmood, Z.H.; Hoq, M.; Rahman, M.H. Investigation of the impact of different ARC layers using PC1D simulation: Application to crystalline silicon solar cells. *J. Theor. Appl. Phys.* **2018**, *12*, 327–334. [CrossRef]
18. Sharma, R. Silicon nitride as antireflection coating to enhance the conversion efficiency of silicon solar cells. *Turk. J. Phys.* **2018**, *42*, 350–355. [CrossRef]
19. Wright, D.N.; Marstein, E.S.; Holt, A. Double layer anti-reflective coatings for silicon solar cells. In Proceedings of the Conference Record of the Thirty-First IEEE Photovoltaic Specialists Conference, Lake Buena Vista, FL, USA, 3–7 January 2005; IEEE: Piscataway, NJ, USA, 2005; pp. 1237–1240.
20. Clugston, D.; Basore, P. PC1D version 5: 32-bit solar cell modeling on personal computers. In Proceedings of the 26th IEEE Photovoltaic Specialists Conference, Anaheim, CA, USA, 29 September–3 October 1997; pp. 207–210.
21. Thirunavukkarasu, G.S.; Seyedmahmoudian, M.; Chandran, J.; Stojcevski, A.; Subramanian, M.; Marnadu, R.; Alfaify, S.; Shkir, M. Optimization of Mono-Crystalline Silicon Solar Cell Devices Using PC1D Simulation. *Energies* **2021**, *14*, 4986. [CrossRef]
22. Wan, Y.; McIntosh, K.R.; Thomson, A.F. Characterisation and optimisation of PECVD SiNx as an antireflection coating and passivation layer for silicon solar cells. *AIP Adv.* **2013**, *3*, 032113. [CrossRef]
23. Siqueiros, J.M.; Machorro, R.; Regalado, L.E. Determination of the optical constants of MgF_2 and ZnS from spectrophotometric measurements and the classical oscillator method. *Appl. Opt.* **1988**, *27*, 2549–2553. [CrossRef]
24. Edward, D.P.; Palik, I. *Handbook of Optical Constants of Solids*; Academic Press: Cambridge, MA, USA, 1985.
25. Johnson, C.M.; Conibeer, G.J. Limiting efficiency of generalized realistic c-Si solar cells coupled to ideal up-converters. *J. Appl. Phys.* **2012**, *112*, 103108. [CrossRef]
26. Cox, J.T.; Hass, G. Antireflection coatings for optical and infrared materials. *Phys. Thin Film.* **1968**, *2*, 239.
27. Balaji, N.; Nguyen, H.T.T.; Park, C.; Ju, M.; Raja, J.; Chatterjee, S.; Jeyakumar, R.; Yi, J. Electrical and optical characterization of SiOxNy and SiO_2 dielectric layers and rear surface passivation by using SiO_2/SiOxNy stack layers with screen printed local Al-BSF for c-Si solar cells. *Curr. Appl. Phys.* **2018**, *18*, 107–113. [CrossRef]
28. Balaji, N.; Lee, S.; Park, C.; Raja, J.; Nguyen, H.T.T.; Chatterjee, S.; Nikesh, K.; Jeyakumar, R.; Yi, J. Surface passivation of boron emitters on n-type c-Si solar cells using silicon dioxide and a PECVD silicon oxynitride stack. *RSC Adv.* **2016**, *6*, 70040–70045. [CrossRef]
29. Lee, Y.; Gong, D.; Balaji, N.; Lee, Y.J.; Yi, J. Stability of SiN X/SiN X double stack antireflection coating for single crystalline silicon solar cells. *Nanoscale Res. Lett.* **2012**, *7*, 50. [CrossRef]